



ELSEVIER

Journal of Crystal Growth 204 (1999) 419–428

JOURNAL OF **CRYSTAL
GROWTH**

www.elsevier.nl/locate/jcrysgro

Morphological and structural characteristics of homoepitaxial GaN grown by metalorganic chemical vapour deposition (MOCVD)

J.L. Weyher^{a,b,*}, P.D. Brown^{c,1}, A.R.A. Zauner^a, S. Müller^d, C.B. Boothroyd^c,
D.T. Foord^c, P.R. Hageman^a, C.J. Humphreys^c, P.K. Larsen^a, I. Grzegory^b,
S. Porowski^b

^a*Exp. Solid State Physics III, RIM, University of Nijmegen, Toernooiveld 1, 6525 ED Nijmegen, The Netherlands*

^b*High Pressure Research Centre, Polish Academy of Sciences, ul. Sokolowska 29/37, P-01142 Warsaw, Poland*

^c*Department of Materials Sciences and Metallurgy, University of Cambridge, Pembroke Street, Cambridge CB2 3QZ, UK*

^d*Fraunhofer-Institut für Angewandte Festkörperphysik, Tullastrasse 72, 79108 Freiburg, Germany*

Received 18 January 1999; accepted 18 April 1999

Communicated by J.B. Mullin

Abstract

MOCVD-grown GaN on the N-polar surface of GaN substrates has been found to exhibit gross hexagonal pyramidal features (typically 10–50 μm in size depending on layer thickness). The evolution of the pyramidal defects is dominated by the growth rate of an emergent core of inversion domain (typically 100 nm in size). The inversion domains nucleate at a thin band of oxygen containing amorphous material (2–5 nm in thickness), being remnant contamination from the mechano-chemical polishing technique used to prepare the substrates prior to growth. Apart from pyramidal hillocks, the flat-topped hillocks are also formed. The arguments are presented on the association between these features and the core dislocations, which constitute the source of the growth steps. Improvement in the substrate polishing procedures allowed the effective elimination of these surface hillocks. © 1999 Elsevier Science B.V. All rights reserved.

PACS: 68.55; 68.35

Keywords: Gallium nitride; Epitaxial layers; Defects; Transmission electron microscopy

1. Introduction

Despite the remarkable progress which has been made in the last decade in growing morphologically good hetero-epitaxial GaN layers, this material still shows a very high density of diverse defects. In particular, dislocations, inversion domains (IDs), nano-pipes and surface pits are of

* Corresponding author. Tel.: + 31-24-3652584; fax: + 31-24-3652314.

E-mail address: jlw@sci.kun.nl (J.L. Weyher)

¹ Now at: Department of Materials Engineering and Materials Design, University of Nottingham, University Park, Nottingham NG7 2RD, UK.

continued concern to crystal growers, see e.g. Refs. [1–6]. For high-power optoelectronic and elevated-temperature device applications, the present structural characteristics of hetero-epitaxial GaN seem to be insufficient. It has been shown that dislocations in GaN epitaxial layers do indeed have nonradiative and recombinative properties [7–10], and the indication is that dislocations in GaN behave during photo-etching in a similar fashion to those in GaAs; i.e. they constitute very effective recombination sites for photo-generated carriers [11] and are the reason for the formation of hillocks at the outcrop of dislocations instead of etch pits. At the same time, micro- and nano-pipes which are commonly observed in hetero-epitaxial GaN layers might become “killer defects” for the electrical properties, as has been shown for SiC-based p–n junction devices [12].

In order to obtain low defect density device structures, a variety of substrate, and hybrid substrate, preparation techniques are presently being considered including: (i) the technique of epitaxial lateral overgrowth (ELOG) [13,14], (ii) the use of hydride vapour-phase epitaxy (HVPE) to grow thick GaN layers followed by the lift-off technique to provide large area GaN substrates [15,16] and (iii) the growth of single crystal GaN under a high hydrostatic pressure of nitrogen [17]. In the context of this third case, it has been reported that bulk plate-like GaN crystals with etch pit density (EPD) below $1 \times 10^2 \text{ cm}^{-2}$ can be reproducibly grown, with size up to 12 mm, which makes them attractive as substrates for high-power laser structures. Up to now, attempts at GaN homo-epitaxial growth on as-grown or mechanically polished single-crystal substrates by MOCVD and MBE [18–20] have led to two important conclusions. Firstly, the epitaxial layers retain the polarity of the substrates and secondly, defects emanating from the epilayer/substrate interface arise due to existing or processing induced surface inhomogeneities. However, the recent application of a mechano-chemical polishing method to the N-polar (0 0 0 $\bar{1}$) surface of GaN bulk crystals has enabled the preparation of epi-ready quality substrates [21]. In the present communication we report on a systematic study of the morphological and structural characteristics of N-polar GaN layers grown by

MOCVD on mechano-chemically polished GaN single crystals.

2. Experimental procedure

The GaN crystals used as substrates for epitaxy in this study were grown under a high-hydrostatic pressure of nitrogen (15–20 kbar) from liquid gallium at a temperature of 1600°C [17]. Both sides of the {0 0 0 1} oriented plate-like crystals were mechanically polished using 0.1 μm grade diamond paste, while the (0 0 0 $\bar{1}$) N-faces (polarity assignment according to Refs. [22–24]) were subsequently mechano-chemically polished in an aqueous solution of KOH following the procedure described in Ref. [21]. Undoped epitaxial GaN layers were grown in a horizontal reactor by the metalorganic chemical vapour deposition (MOCVD) method. The crystals were heated up to the growth temperature of 1050°C under a N_2/NH_3 atmosphere. Epitaxial growth was performed using trimethylgallium (TMG) and NH_3 precursors with H_2 as the carrier gas, under a total pressure of 50 mbar. The TMG flow rate was about 60 $\mu\text{mol}/\text{min}$ and the NH_3 flow was 2.5 standard litre/min (slm), diluted with H_2 to a total flow of 5 slm. The time of epitaxial growth was 1 h, unless denoted otherwise (for the case of one sample considered here). Using this procedure high-quality GaN epitaxial layers have been previously grown reproducibly on sapphire substrates [25]. A range of complementary techniques were used for the morphological and structural characterisation of the epitaxial layers including differential interference contrast (DIC) optical microscopy, scanning electron microscopy (SEM), atomic force microscopy (AFM) and transmission electron microscopy (TEM). The techniques of conventional and high-resolution electron microscopy were complemented by convergent beam electron diffraction (CBED), high angle annular dark field (HAADF) imaging and electron energy loss spectroscopy (EELS). Plan view TEM specimens were prepared by sequential mechanical polishing and conventional Ar ion milling, while focused ion beam (FIB) techniques were used to prepare site specific cross-sectional foils through chosen growth features.

3. Experimental results

Optical examination of the homoepitaxial GaN layers revealed numerous growth hillocks covering almost the entire substrate surface, e.g. Fig. 1a. The size of the hexagonal base of the hillocks was in the range 10–50 μm after 1 h of growth, with density in the range $0.5\text{--}2 \times 10^5 \text{ cm}^{-2}$. The distribution of hillocks was typically nonuniform across each layer surface, with some local regions being free of these macroscopic growth features. This result is based on an examination of ten separate growth runs performed under nominally the same growth conditions. The majority of hillocks assume the shape

of regular point-topped pyramids (denoted by H_p in Figs. 1a and b), although some of them are macroscopically flat-topped or disrupted (denoted H_f and H_d in Fig. 1b).

Close inspection of the point-topped hexagonal hillocks using AFM reveals morphological details of the core on the nanometer scale. In particular, the highest and most well-defined pyramids (arrowed in Fig. 1a) are terminated by sub-micron sized flat hexagonal cores, as shown in Fig. 2a. The AFM analysis shows that these flat regions are atomically smooth, i.e. with roughness in the range 0.1–0.15 nm, which, being below the atomic step size, is merely evidence of background noise

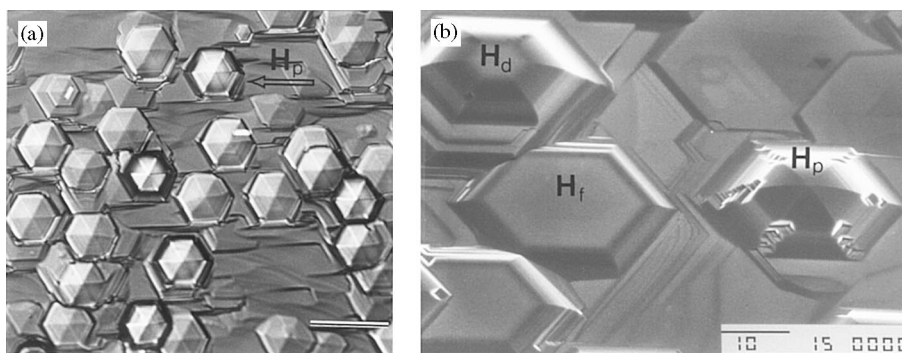


Fig. 1. (a) Differential interference contrast optical micrograph of MOCVD-grown homoepitaxial GaN on an N-polar substrate, with point-topped (H_p) pyramids. (b) SEM image of flat-topped (H_f) and disrupted (H_d) hexagonal hillocks. The marker represents 100 μm .

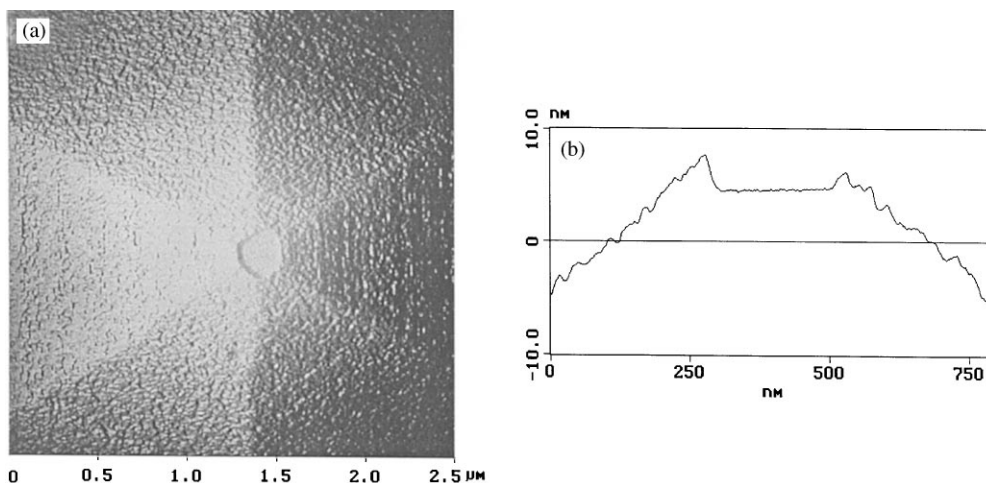


Fig. 2. (a) AFM image and (b) line profile across the top of an hexagonal pyramidal hillock (arrowed in Fig. 1a), terminated by a 100 nm sized flat-topped region.

from the AFM procedure. Some of these flat cores were bounded by material with a noticeably rougher surface morphology, as demonstrated by Fig. 2b. The presence of this type of termination is typical only of the highest pyramidal hillocks, which constitute about 20% of the whole population of these features. The macroscopically flat-topped hillocks are also flat on the nm scale, with AFM data indicating height fluctuations of only 0.5–1 nm (i.e.

on the order of the atomic layer thickness), as shown in Figs. 3a and b. There is also the suggestion of the emergence of dislocations in the centre of such hillocks, as evidenced by the atomic-size steps shown in Figs. 4a and b, while some exhibit a needle-shaped tip at the centre, as shown by Fig. 5a. For the case of this type of growth feature, the tip seems to serve as a source of atomic layer surface steps (Fig. 5b), by which step flow growth is mediated.

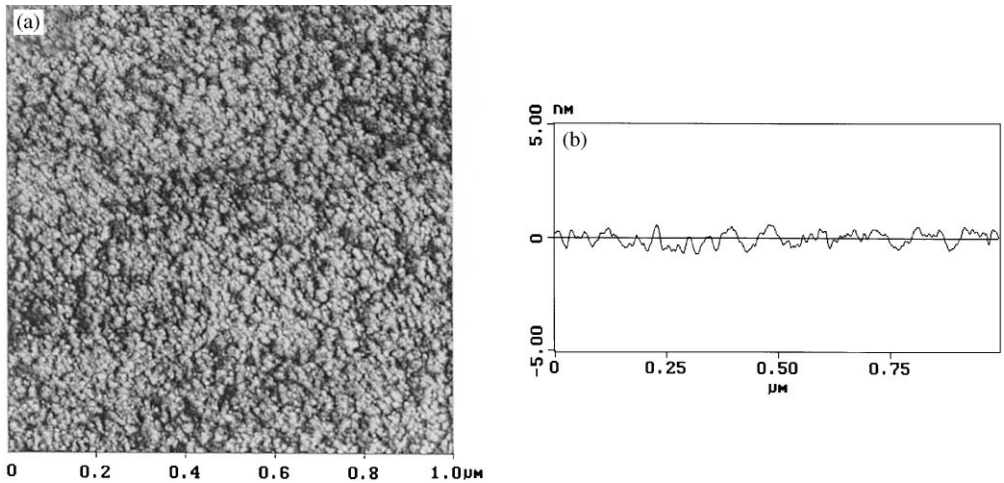


Fig. 3. (a) AFM image and (b) line profile taken across the centre of a macroscopically flat hexagonal hillock (denoted H_f in Fig. 1b).

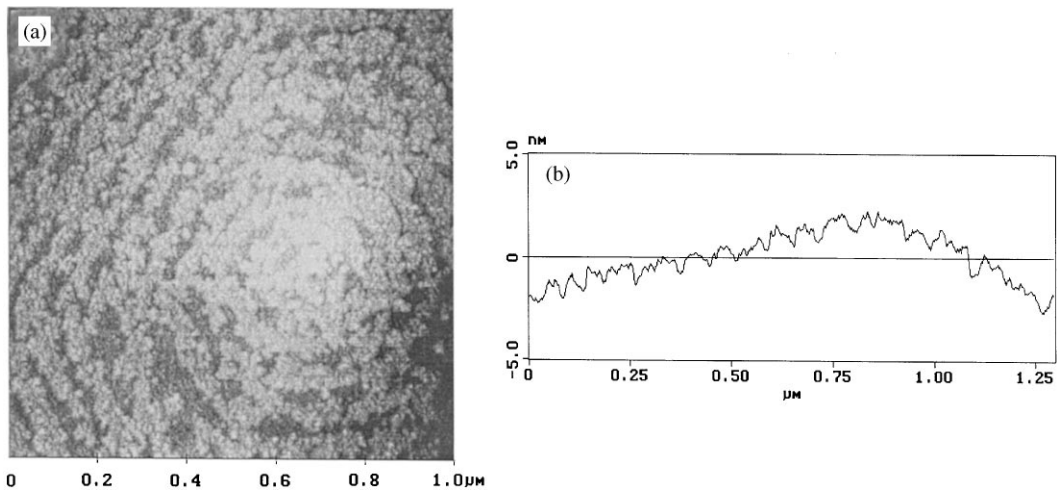


Fig. 4. (a) AFM image and (b) line profile taken at the centre of a macroscopically flat hillock.

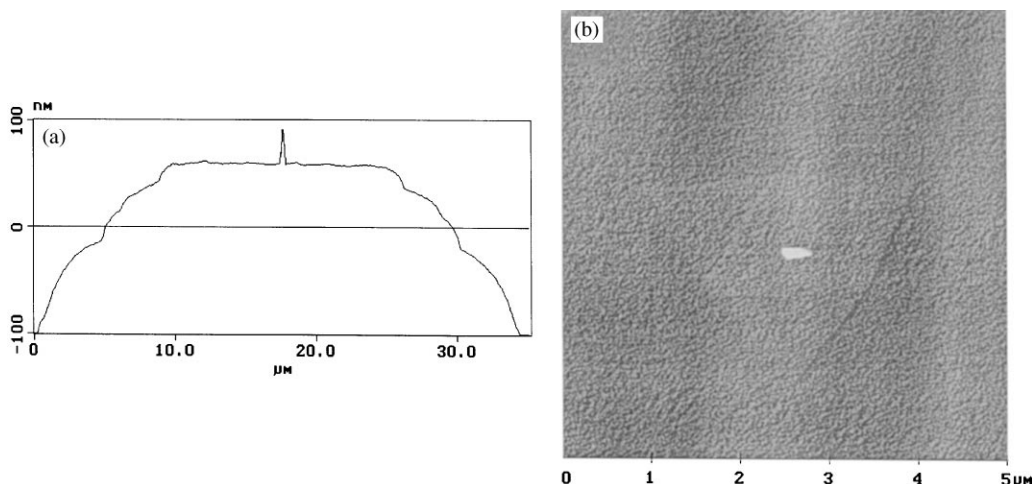


Fig. 5. (a) AFM section and (b) surface image taken at the centre of a macroscopically flat hillock.

The material between the growth hillocks also exhibits characteristic step flow growth, with approx. 1 nm step heights, as revealed by AFM (Fig. 6a). Also, the matrix surface between these flow steps is not atomically smooth, being covered by clusters with height differences of the order of one atomic layer (Figs. 6b and c).

In order to reveal the nature and origin of the defects responsible for the formation of the hexagonal hillocks, both plan view and cross-sectional TEM specimens were prepared from an epitaxial layer grown for 15 min. Choosing to section into a thin layer increased the chances of hitting a nucleation source, since any small deviation in orientation of the layer when sectioned using FIB can result in a sub-surface target (approx. 100 nm in size in this instance) being missed. By inspection of the large tilt plan view TEM images, it appeared that the pyramidal growth hillocks exhibit faceted core structures, without any other threading defects. Cross-sectional TEM specimens were thus prepared precisely through the cores of the hexagonal growth hillocks using the FIB technique for more detailed structural analysis. TEM examination revealed columnar defects located just below the apex of each hillock, as illustrated by Fig. 7a. The column emanates from a platelet of approx. 100 nm size, which is presumed to delineate the original epilayer/substrate interface (Fig. 7b). No

other sign of the interface plane was evident from these diffraction contrast images. The striped nature of the columnar defect (Figs. 7a and b) is simply related to the fact that these are projected images of an irregular hexagonal column of material. Precise analysis of this columnar defect and the clarification of its nucleation site required further sequential thinning of the sample and the application of a range of complementary TEM procedures. In particular, asymmetries within CBED $\{0002\}$ diffraction discs allowed the polar nature of the material to be unambiguously identified [26–28]. The image and diffraction patterns were corrected for image rotation (using a polarity calibrated reference sample). Then, regard was given to the variation in contrast of CBED $\{0002\}$ discs with increasing sample foil thickness [29]. The CBED patterns of Fig. 8 thus demonstrated unequivocally that the epilayer retained the N polarity of the substrate, while the columnar defects exhibit a Ga surface polarity, thereby confirming them to be inversion domains (ID). HAADF (otherwise termed Z-contrast) imaging using a dedicated STEM demonstrated that a band of low atomic number material (giving dark contrast as compared with the GaN matrix) constituted the nucleation site. The HRTEM image in Fig. 9a shows a fragment of this planar nucleus thinned to a level such that it is free of any matrix material in the projected

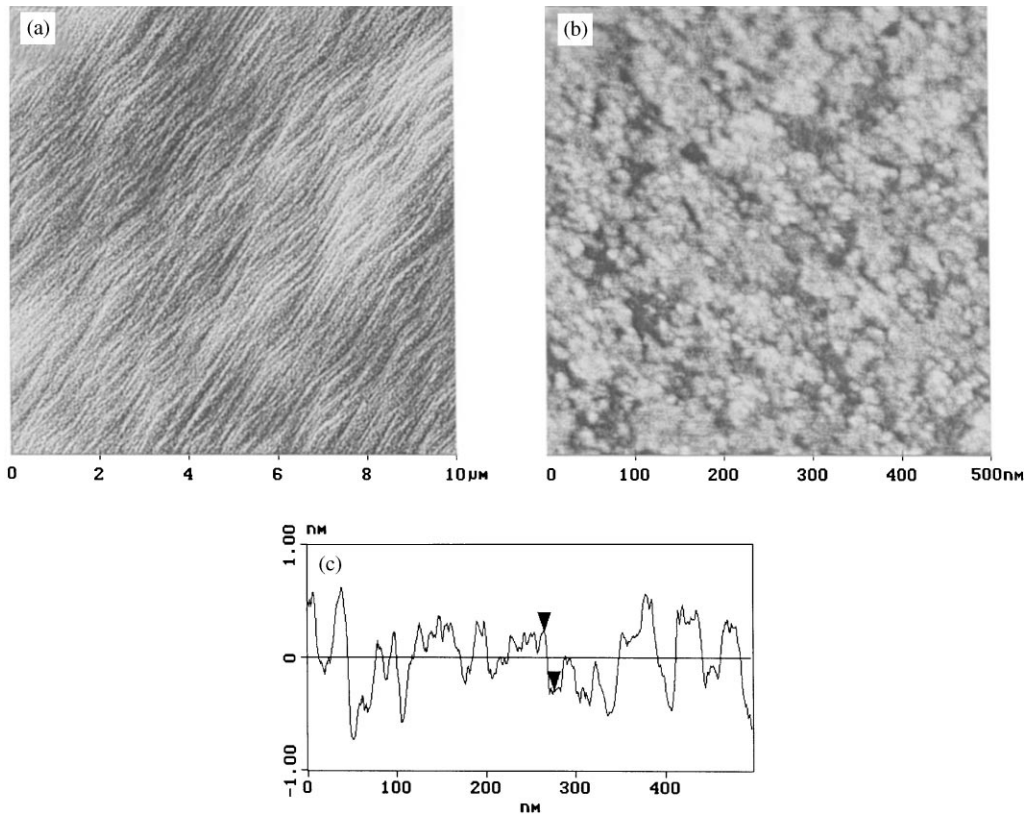


Fig. 6. (a–c) AFM images and profile across the matrix of the homoepitaxial layer between the hexagonal hillocks: (b) shows evidence for surface structure between the steps, while (c) shows the corresponding line profile.

image of the nucleation site. This confirms the nucleation site to consist of a band of amorphous material, 2–5 nm in thickness, rather than being due to a distinct crystallographic defect. Finally EELS clearly shows a marked increase in the oxygen concentration and drop in the nitrogen concentration being associated with the source of the ID, when compared with nearby regions of the GaN matrix (Fig. 9b). Further details on the application of these complementary TEM techniques to the analysis of these nucleation sites will be presented in a separate paper [30].

Some of the growth hillocks show morphological perturbations at the edges of the hexagonal pyramids, as indicated by H_p in Fig. 1b. Cross-sectional TEM examination of one such hillock reveals the presence of three defects, which appar-

ently initiate at a common origin located outside the plane of the thin foil in this instance (Fig. 10). Since this epitaxial layer was grown under standard conditions, i.e. for 1 h, and the thickness of the epilayer was above 3 μm , it was difficult to obtain the full extent of these threading defects totally within the plane of a TEM specimen. Apart from the ID at the core of the growth hillock, one screw dislocation D (presumably situated at the GaN/GaN interface) and an inclined stacking fault (SF) are present. The complex contrast of the ID arises due to its partial removal from the TEM foil by the preparation procedure. The morphological nature of this hillock and the inclination of the SF supports the view that the perturbations observed at the edge of the growth pyramids arise due to the emergence of such SFs out of the layer growth surface.

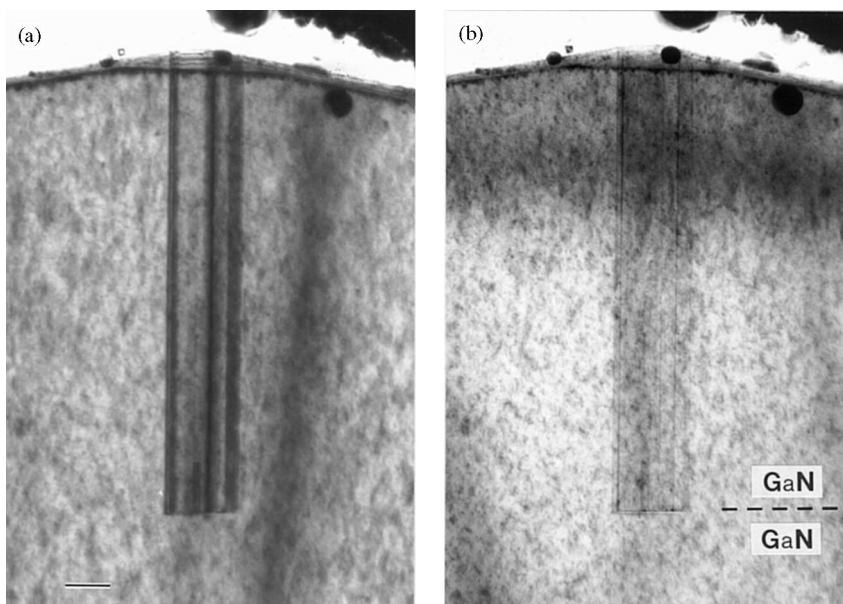


Fig. 7. TEM cross-sectional images of the columnar defect delineating the core of the hexagonal growth hillock (denoted H_p in Fig. 1). (a) Defect imaged with g in the growth direction close to the $\langle 1\bar{1}00 \rangle$ zone, (b) weak beam image of the same defect revealing a thin planar nucleating site at the base of the column. The marker represents 100 nm.

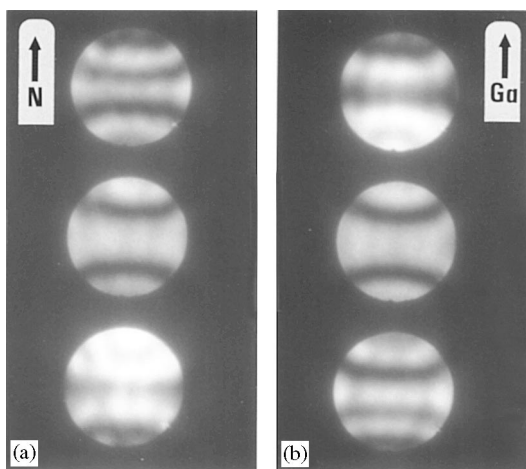


Fig. 8. CBED patterns recorded (a) from the epitaxial matrix and (b) from the columnar defect shown in Fig. 7 confirms the presence of an inversion domain.

TEM sectioning through a macroscopically flat-topped hillock failed to reveal any structural defects, neither threading the layer nor delineating the GaN/GaN interface.

4. Discussion

The evidence confirms that the hexagonal pyramidal hillocks, which form during the MOCVD homoepitaxial growth on N-polar GaN, are due to the presence of inversion domains. Indeed, similar growth defects have been observed in heteroepitaxial N-polar GaN, see e.g. Refs. [5,28,31–33]. The Ga-polar cores of such IDs are found to grow at a higher rate than the surrounding N-polar matrix, and as such are responsible for the formation and propagation of the pyramidal hillocks [5,28]. Our TEM results confirm this conclusion, while the AFM results indicate that the IDs constitute very effective nucleation site for atomic layer surface steps during homoepitaxy. This factor is possibly related to the effect of “overgrowth” of some of the IDs (see Fig. 2b) by the GaN matrix, whereby macroscopically flat-topped hillocks of differing but lower height are formed, presumably containing short segments of ID inside. Overgrowth then explains the presence of hillocks that show macroscopically flat surfaces free of step-flow

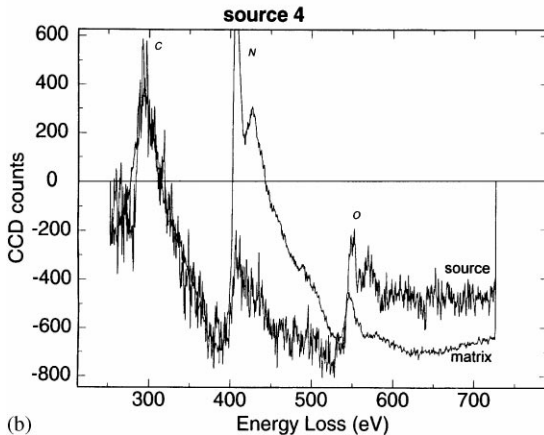
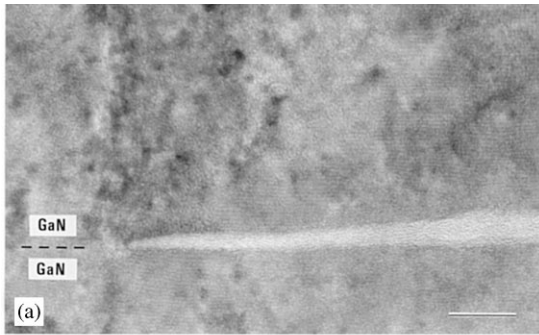


Fig. 9. (a) HREM image of an amorphous band comprising the nucleation site of an ID. The marker represents 10 nm. (b) EELS data recorded from the amorphous band and the matrix showing the association of oxygen with nucleating site.

features (see Fig. 3) and without any dislocations. Such a conclusion is supported by evidence for numerous ID termination events within heteroepitaxial GaN layers [5].

However, when the Ga-polar surface of an ID propagates, essentially pulling up the pyramid around it, the growth rates of opposite polar $(0001)A$ and $(000\bar{1})B$ surfaces means $V_{Ga} > V_N$. This result is consistent with other TEM studies of the heteroepitaxial growth of N-polar GaN [5,34], but contradicts the inference presented in Refs. [4,19,26]. Similar contradictions have also been reported for the vapour-phase epitaxy of different III–V compounds when growth rates are compared on the opposite polar $\{111\}A$ and $\{\bar{1}\bar{1}\bar{1}\}B$ surfaces, see e.g. Refs. [35–37]. In fact, no unequivocal general relationship between the growth rates on

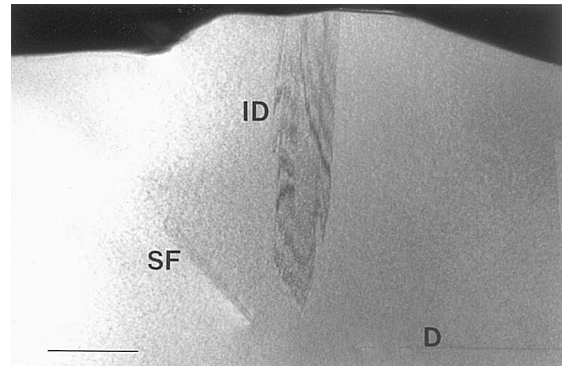


Fig. 10. Bright field TEM image of the centre of a perturbed growth hillock, similar to the one marked H_p in Fig. 1b, showing an inversion domain core (ID), a screw dislocation (D) delimiting the original line of the epilayer/substrate interface and an inclined stacking fault (SF). The marker represents 1 μ m.

polar surfaces of GaN can be deduced based on recent studies of heteroepitaxial GaN [38–40].

The AFM measurements show that the $(0001)Ga$ face of GaN is more stable than the $(000\bar{1})N$ face during epitaxial growth and/or cool down after growth, from comparison of the surface roughness of the Ga-polar surface of the ID and the N-polar surface of the matrix in Fig. 2a, Fig. 3b and Fig. 6b, respectively. Due to the lower stability of the N-polar surface, as compared with the Ga-polar surface, it is suggested that a permanent competition between adsorption and decomposition rates occurs during growth (alternatively, enhanced decomposition occurs during cooling) on the N-polar surface, resulting in a higher atomic-scale roughness and lower average growth rate from the matrix.

Based on the experimental evidence of this study it is difficult to explain the diverse efficiency of IDs in the nucleation of surface steps. Indeed, it is not understood why some of the IDs emerge clear of the interrupted hillocks and yet emanate only singular steps, as shown by Fig. 5. On the other hand, it is evident that some of the flat-topped hillocks are growing due to the presence of dislocations. The height of 0.5 nm surface step, as estimated from Fig. 4b, suggests that the most probable dislocation type which could be the source of these steps is either one pure screw dislocation ($b = \langle 0001 \rangle$) or

a set of even number of partial screw dislocations ($b = \frac{1}{2}\langle 0001 \rangle$). Both types of dislocations were found by TEM in the faceted hexagonal growth islands comprising GaN heteroepitaxial layers [2]. The source of steps shown in Fig. 4a is in fact cooperating with the second one, as recorded by a $5 \times 5 \mu\text{m}$ AFM mapping. Therefore, it can be concluded that the steps of 0.5 nm height are formed due to the presence of two partial screw dislocations with $b = \frac{1}{2}\langle 0001 \rangle$.

The striking evidence of the nucleation of Ga-polar IDs on the 2–5 nm planar amorphous bands of oxygen containing material may be explained in terms of the high adsorption affinity of Ga to O atoms. We presume that the oxygen-containing residue is gallium hydroxide (a likely reaction product of the KOH etch used in the chemo-mechanical polishing of the GaN prior to growth [21]), in keeping with an hemispherically scanned X-ray photoelectron diffraction (HSXPD) study of the factors determining the polarity of epitaxial GaN films on sapphire [22]. This reasoning is supported by a remarkable decrease in the density of hillocks when a modified mechano-chemical treatment of the N-polar substrates is employed. A more detailed systematic study of this subject is presently being performed and will be reported elsewhere.

5. Concluding remarks

The reproducible homoepitaxial MOCVD growth of GaN layers has been achieved on N-polar (000 $\bar{1}$) bulk single-crystal substrates subjected to a mechano-chemical polish in KOH aqueous solution. Hexagonal pyramids and flat-topped hillocks of density 10^5 cm^{-2} are the predominant defects formed, and these are attributed to the nucleation of IDs at distributed 100 nm amorphous bands of oxygen containing material, typically 2–5 nm thick, remnant from the polishing process. TEM analysis confirms the presence of Ga-polar IDs embedded within the N-polar matrix of the epilayer, it follows that the growth rate is higher on the Ga-polar surface. The lower growth rate on the N-polar matrix surface is attributed to the lower stability of this surface. Between the hillocks, the epitaxial layers grow in accordance with a step flow

mechanism, with step heights of 0.5–1 nm. There is perfect matching of the lattice at the substrate/epilayer interface since no discontinuity delineating the interface could be discerned during TEM examination.

Acknowledgements

J.L.W. wishes to thank NATO Scientific Affairs Division for the Grant HTECH: LG 972924. This work was financially supported by the Dutch Technology Foundation (STW).

References

- [1] L.T. Romano, J.E. Northrup, M.A. O'Keefe, *Appl. Phys. Lett.* 69 (1996) 2394.
- [2] S. Christiansen, M. Albrecht, W. Dorsch, H.P. Strunk, A. Pelzmann, M. Mayer, M. Kamp, K.J. Ebeling, C. Zanotti-Fregonara, G. Salviati, *Mater. Sci. Eng. B* 43 (1997) 296.
- [3] Y. Xin, P.D. Brown, C.J. Humphreys, T.S. Cheng, C.T. Foxon, *Appl. Phys. Lett.* 70 (1997) 1308.
- [4] Z. Liliental-Weber, Y. Chen, S. Ruvimov, J. Washburn, *Phys. Rev. Lett.* 79 (1997) 2835.
- [5] J.L. Rouvière, M. Arlery, R. Niebuhr, K.H. Bachem, O. Briot, *Mater. Sci. Eng. B* 43 (1997) 161.
- [6] J. Elsner, R. Jones, M. Haugk, R. Gutierrez, Th. Frauenheim, M.I. Heggie, S. Öberg, P.R. Briddon, *Appl. Phys. Lett.* 73 (1998) 3530.
- [7] S.J. Rosner, E.C. Carr, M.J. Ludowise, G. Girolami, H.I. Erikson, *Appl. Phys. Lett.* 70 (1997) 420.
- [8] F. Bertram, J. Christen, M. Schmidt, M. Topf, S. Koymov, S. Fischer, B. Meyer, *Mater. Sci. Eng. B* 50 (1997) 165.
- [9] C. Youtsey, L.T. Romano, I. Adesida, *Appl. Phys. Lett.* 73 (1998) 797.
- [10] T. Sugahara, H. Sato, M. Hao, Y. Naoi, S. Kurai, S. Tattori, K. Yamashita, K. Nishino, L.T. Romano, S. Sakai, *Jpn. J. Appl. Phys.* 37 (1998) L398.
- [11] J.L. Weyher, *Inst. Phys. Conf. Ser. No. 146*, IOP Publishing Ltd., Amsterdam, 1995, p. 399.
- [12] P.G. Neudeck, J.A. Powell, *IEEE Electron. Device Lett.* 15 (1994) 63.
- [13] X. Li, A.M. Jones, S.D. Roh, D.A. Turnbull, S.G. Bishop, J.J. Coleman, *J. Electron. Mater.* 26 (1996) 306.
- [14] S. Nakamura, M. Senoh, S. Nagahama, N. Iwasa, T. Yamada, T. Matsushita, H. Kiyoku, Y. Sugimoto, T. Kozaki, H. Umemoto, M. Sano, K. Chocho, *Appl. Phys. Lett.* 72 (1998) 2014.
- [15] S.T. Kim, Y.J. Lee, D.C. Moon, C.H. Hong, T.K. Yoo, *J. Crystal Growth* 194 (1998) 37.

- [16] R.J. Molnar, W. Götz, L.T. Romano, N.M. Johnson, *J. Crystal Growth* 178 (1997) 147.
- [17] S. Porowski, *J. Crystal Growth* 166 (1996) 583.
- [18] F.A. Ponce, D.P. Bour, W. Götz, N.M. Johnson, H.I. Helava, I. Grzegory, J. Jun, S. Porowski, *Appl. Phys. Lett.* 68 (1996) 917.
- [19] Z. Liliental-Weber, J. Washburn, K. Pakula, J. Baranowski, *Microsc. Microanal.* 3 (1997) 436.
- [20] J.M. Baranowski, Z. Liliental-Weber, K. Korona, K. Pakula, R. Stepniewski, A. Wyszomolek, I. Grzegory, G. Nowak, S. Porowski, B. Monemar, P. Bergman, *Mater. Res. Soc. Symp. Proc. Vol. 449*, MRS, 1997, p. 393.
- [21] J.L. Weyher, S. Müller, I. Grzegory, S. Porowski, *J. Crystal Growth* 182 (1997) 17.
- [22] M. Seelmann-Eggebert, J.L. Weyher, H. Obloh, H. Zimmermann, A. Rar, S. Porowski, *Appl. Phys. Lett.* 71 (1997) 2635.
- [23] E.S. Hellman, *MRS Nitride Semiconductor Research*, MIJ-NSR Vol. 3, Article 11, 1998.
- [24] J.L. Rouvière, J.L. Weyher, M. Seelmann-Eggebert, S. Porowski, *Appl. Phys. Lett.* 73 (1998) 668.
- [25] F.K. de Theije, A.R.A. Zauner, P.R. Hageman, W.J.P. van Enkevort, P.K. Larsen, *J. Crystal Growth* 197 (1999) 37.
- [26] Z. Liliental-Weber, C. Kisielowski, S. Ruvimov, Y. Chen, J. Washburn, I. Grzegory, M. Bockowski, J. Jun, S. Porowski, *J. Electron. Mater.* 25 (1996) 1545.
- [27] P. Vermaut, P. Ruterana, G. Nouet, *Phil. Mag. A* 76 (1997) 1215.
- [28] J.L. Rouvière, M. Arlery, A. Bourret, *Inst. Phys. Conf. Ser. No. 157*, IOP Publishing Ltd., Amsterdam, 1997, p. 173.
- [29] D. Cherns, W.T. Young, M. Saunders, J.W. Steeds, F.A. Ponce, S. Nakamura, *Phil. Mag. A* 77 (1998) 273.
- [30] P.D. Brown, J.L. Weyher, C.B. Boothroyd, D.A. Foord, A.R.A. Zauner, P.R. Hageman, P.K. Larsen, M. Bockowski, C.J. Humphreys, XI MSM Conf., 1999, submitted for publication.
- [31] I. Akasaki, H. Amano, Y. Koide, K. Hiramatsu, N. Sawaki, *J. Crystal Growth* 98 (1989) 209.
- [32] O. Briot, J.P. Alexis, M. Tchounkeu, R.L. Aulombard, *Mater. Sci. Eng. B* 43 (1997) 147.
- [33] B. Péc̄z, M.A. di Forte-Poisson, L. Toth, G. Radnoczi, G. Huhn, V. Papaioannou, J. Stoemenos, *Mater. Sci. Eng. B* 50 (1997) 93.
- [34] B. Daudin, J.L. Rouvière, M. Arlery, *Mater. Sci. Eng. B* 43 (1997) 157.
- [35] R.E. Ewing, P.E. Green, *J. Electrochem. Soc.* 111 (1964) 1266.
- [36] K. Kamon, M. Shimazu, K. Kimura, M. Mihara, M. Ishii, *J. Crystal Growth* 84 (1987) 126.
- [37] R. Bhat, C. Caneau, C.E. Zah, M.A. Koza, W.A. Bonner, D.M. Hwang, S.A. Schwarz, S.G. Menocal, F.G. Favire, *J. Crystal Growth* 107 (1991) 772.
- [38] M. Nagahara, S. Miyoshi, H. Yaguchi, K. Onabe, Y. Shiraki, R. Ito, *J. Crystal Growth* 145 (1994) 197.
- [39] CH Hong, K. Wang, D. Pavlidis, *J. Electron. Mater.* 24 (1995) 213.
- [40] J.W. Yang, J.N. Kuznia, Q.C. Chen, M. Asif Khan, T. George, M. De Graef, S. Mahajan, *Appl. Phys. Lett.* 67 (1995) 3759.